

Synergistic interaction between phage therapy and antibiotics clears *Pseudomonas aeruginosa* infection in endocarditis and reduces virulence

Frank Oechslin,^{a#} Philippe Piccardi,^a Stefano Mancini,^a Jérôme Gabard,^b Philippe Moreillon,^a José M. Entenza,^a Gregory Resch,^a Yok-Ai Que^c

Dept. of Fundamental Microbiology, University of Lausanne, Switzerland^a;
Pherecydes Pharma, Romainville, France^b; Dept. of Intensive Care Medicine, Bern University Hospital, Switzerland^c.

Running Head: Phage therapy for *Pseudomonas* endocarditis

#Address correspondence to Frank Oechslin, Frank.Oechslin@gmail.ch. University of Lausanne, Quartier UNIL-Sorge, Bâtiment Biophore, CH-1015 Lausanne, Switzerland.

Y-A.Q. and G.R. contributed equally to this work.

Abstract: 200 words

Text: 1492 words

Key words: bacteriophage, phage therapy, endocarditis, *Pseudomonas aeruginosa*, resistance, antibiotic.

Abstract

BACKGROUND:

Increasing antibiotic resistance warrants therapeutic alternatives. Here we investigated the efficacy of bacteriophage-therapy (phage) alone or combined with antibiotics against experimental endocarditis (EE) due to *Pseudomonas aeruginosa*, an archetype of difficult-to-treat infection.

METHODS:

In vitro fibrin-clots and rats with aortic EE were treated with an anti-pseudomonas phage cocktail alone or combined with ciprofloxacin. Phage pharmacology, therapeutic efficacy, and resistance were determined.

RESULTS:

In vitro, single-dose phage-therapy killed 7 log CFU/g of fibrin-clots in 6 h. Phage-resistant mutants regrew after 24 h, but were prevented by combination with ciprofloxacin (2.5xMIC). *In vivo*, single-dose phage-therapy killed 2.5 log CFU/g of vegetations in 6 h ($P < 0.001$ versus untreated controls) and was comparable to ciprofloxacin monotherapy. Moreover, phage-ciprofloxacin combinations were highly synergistic, killing >6 log CFU/g of vegetations in 6 h and successfully treating 64% (7/11) of rats. Phage-resistant mutants emerged *in vitro* but not *in vivo*, most likely because resistant mutations affected bacterial surface determinants important for infectivity (e.g. the *pilT* and *galU* genes involved in pilus motility and LPS formation).

CONCLUSION:

Single-dose phage-therapy was active against *P. aeruginosa* EE and highly synergistic with ciprofloxacin. Phage-resistant mutants had impaired infectivity. Phage-therapy alone or combined with antibiotics merits further clinical consideration.

Introduction

The global increase in antibiotic resistance is reviving the need for alternative antimicrobial strategies, including phage therapy. This “forgotten cure” was developed in parallel to antibiotics during the first half of the 20th century and is still commonly used in countries of the former Soviet Union [1]. However, it was not developed at large scale in Western countries, and information on phage pharmacokinetics/pharmacodynamics (PK/PD), drug interactions, *in vivo* efficacy, and emergence of resistance remains scarce. Phages have been administered by various routes, including inhalation for pneumonia (reviewed in [2]), surgical rinsing for chronic osteomyelitis [3], and intravenous injection for severe systemic infections, such as typhoid fever (reviewed in [4]). However, only few studies provide a comprehensive picture linking phage pharmacology to antibacterial efficacy [5, 6]. Moreover, with few exceptions [6], the emergence of phage resistance is seldom addressed, even in recent clinical studies [7-9].

Detailed understanding of bacterial resistance to phages is critical if phages were to be used more broadly in the clinical setting. Phage-resistant bacteria can result from several mechanisms, including modification of cell-surface receptors, restriction-modification of incoming (foreign) phage DNA, or inter-phage immunity [10]. Resistance mutations may arise spontaneously *in vitro* and are likely to be selected *in vivo* as well [6]. Some mutations may affect LPS (a common phage receptors) and impact bacterial fitness or virulence [11-13]. However, other kinds of mutations or further mutations restoring virulence cannot be excluded and must be scrutinized.

The intrinsic bactericidal properties of anti-infective compounds are most reliably studied in models of “therapeutic sanctuaries”, where natural host defenses are poorly involved. Experimental endocarditis (EE) and experimental meningitis are two

such models. Experimental meningitis implicates a special anatomical setting where drug distribution depends on the blood-brain barrier. In contrast, EE mirrors the general situation encountered in many deep-seated infections. Moreover, endocarditis pathogens surround themselves with amorphous aggregates of platelet-fibrin clots in which cellular host defenses cannot penetrate (for review see [14]). Thus, the capability of antimicrobials to penetrate into vegetations is a critical issue. In the present experiments, we systematically explored the efficacy of a clinically-used anti-pseudomonas phage cocktail (cocktail PP1131 currently investigated in the multicentric Phagoburn clinical trial for treatment of burn-wound infections; <http://www.phagoburn.eu>) in a dual *in vitro* and *in vivo* model of experimental endocarditis due to *P. aeruginosa*.

Phage therapy alone was active both *in vitro* and in animals with EE. Moreover, it was highly synergistic with antibiotics. Although phage-resistant bacteria emerged *in vitro*, they were not detectable *in vivo* due to fitness alteration in the animal milieu. These results suggest that phage therapy alone or combined with antibiotics (in this case ciprofloxacin) deserves further consideration for future clinical application.

Results

***P. aeruginosa* host range of individual phages composing the PP1131 cocktail.**

The 12 phages contained in the PP1131 cocktail were evaluated for their ability to lyse a panel of 33 laboratory and clinical isolates of *P. aeruginosa* from our own collection using spot assays (Supplementary Table 1 and 2). This test showed that 31/33 (94 %) of the *P. aeruginosa* isolates were lysed by at least two phages, whereas only strains PA7 and 10 were resistant to the 12 phages. The relatedness of

the 12 phages regarding strain specificity was further evaluated by hierarchical cluster analysis based on a binary matrix derived from the spot assay. Supplementary Figure 1 indicates that the phages of the cocktail were different from each other regarding to their host specificity profiles, thus ensuring coverage of multiple strains.

Of note, spot assays indicate both lysis-from-within (due to productive phage infection) and lysis-from-without (due to phage attachment only). Therefore, while they assess specificity of phage-bacteria interactions they may underestimate genuine productive infectivity. In the present experiments the PP1331 phage cocktail achieved productive infection in 28/33 (84%) of the tested strains (Supplementary Figure 2).

Activity of the phage cocktail in the *in vitro* fibrin-clot model. The efficacy of the cocktail was tested in fibrin clots simulating endocarditis vegetations [15]. Two *P. aeruginosa* strains were used, namely strain P7, which was not infected by any of the cocktail's phages, and strain CHA which was susceptible to all of them. For resistant strain PA7, no phage-induced killing and no *in situ* phage amplification was observed (Figure 1.A). Moreover, physical disintegration of the clots, possibly due to the action of bacterial proteases, was observed after 24 h (Figure 1.C).

In contrast, a significant loss of bacterial viability of approximately 6 logs CFU/g was observed after 6 h when CHA-infected clots were challenged with the cocktail (Figure 1.B, $p = 0.0001$ compared to the initial bacterial load). Phage-induced killing was accompanied by a phage amplification of 5 log PFU/g of clots ($p = 0.0001$ compared to non-infected clots). In addition, phage-induced bacterial killing prevented bacterial-induced clot disintegration (Figure 1.D), indicating that phages diffused through the

fibrin meshwork and killed bacteria located inside the clots. Yet, the sharp initial phage-induced killing was followed by bacterial regrowth after 24 h (Figure 1.B). This regrowth was caused by the development of phage-resistant bacterial mutants and was not accompanied by further phage amplification.

Frequency of phage resistance in broth cultures and fibrin clots. In the absence of phages, spontaneous resistant mutants occurred at an average frequency of ca. 10^{-7} , and at ca. 10^{-8} against the whole cocktail (result not shown) both in batch cultures and in fibrin clots after 6 h and 24 h (Supplementary Table3, column 2). In contrast, the proportion of phage-resistant bacteria increased sharply after exposure to phages due to the replacement of phage-susceptible bacteria by resistant subpopulations, *i.e.* 10^{-4} at 6 h and 10^{-2} at 24 h (Supplementary Table S3, columns 5 and 6).

Prevention of phage resistance using phage-antibiotic combinations. In order to prevent the development of phage-resistant subpopulations we attempted to combine phages with antibiotics. Combining the phage cocktail with 2.5-times the MIC of ciprofloxacin or meropenem inhibited the regrowth of phage-resistant mutants after 24 h (Figure 2.A and 2.B, dashed dotted lines, respectively). Moreover, the two antibiotics were highly synergistic with phages at 24 h, as defined by a ≥ 3 log CFU/ml decrease in bacterial viable counts when compared to single phage or antibiotic therapy alone.

Phage pharmacokinetics. The pharmacokinetics of the phage cocktail was assessed in the plasma and tissues of non-infected rats with catheter-induced aortic vegetations following a single intravenous (i.v.) bolus injection or during continuous infusion (Figure 3.A, solid and dashed line, respectively). A high plasma titer (8.5 ± 1.5 log PFU/ml) was measured 1 h after bolus injection, followed by a continuous decrease to 4.9 ± 0.6 log PFU/ml at 24 h (elimination half-life = ca. 2.3 h). In parallel, the concentrations of phages in vegetations decreased from 7.5 ± 0.3 to 6.2 ± 0.9 log PFU/g between 6 h and 24 h post administration. A similar tendency was observed in the spleen, kidney, liver, lung and brain (elimination half-life = ca. 9 h, Supplementary Figure 3). This demonstrated phage diffusion into the organs and delayed phage clearance compared to plasma. During continuous infusion, phage titers in plasma progressively increased to reach a plateau of 8.5 ± 0.2 log PFU/ml after 6 h, which is comparable to the concentration achieved after 1 h following bolus injection. Phage concentrations in the vegetations and organs remained high after 24 h (7.4 ± 0.9 log PFU/ml, Supplementary Figure 3).

Treatment of EE. Inoculation with 10^8 CFU of *P. aeruginosa* CHA induced EE with bacterial loads in vegetations of control rats of > 8 log CFU/g 18 h after bacterial challenge (Figure 3.B). Administration of the phage cocktail 18 h after bacterial challenge by either continuous or bolus injection decreased median vegetation bacterial titers by 3.0 and 2.3 log CFU/g, respectively, within 6 h of therapy (Figure 3.B; $p < 0.0001$ compared to treatment onset). No significant difference between the two routes of administration was observed. Notably, a single bolus injection of ciprofloxacin simulating a single oral dose of 750 mg in adults [16] decreased median vegetation bacterial titers by 2.6 log CFU/g (Figure 3.B), which was comparable to

phage therapy. Moreover, the combination of phages with ciprofloxacin was highly synergistic, resulting in negative vegetation cultures in 7/11 rats receiving combined therapy after 6 h, as compared to 0/28 in phage-alone or ciprofloxacin-alone treated groups (Figure 3.B; $p < 0.005$). Likewise, the residual median vegetation bacterial titers of ≤ 2 log CFU/g in the combined therapy group were significantly lower than the ≥ 6 log CFU/g titers detected in the monotherapy groups ($p < 0.0001$).

***In situ* penetration of phages in valve tissues.** Optical microscopy and transmission electron microscopy (TEM) were performed on vegetation samples in order to visualize the presence and activity of phages inside the vegetations. Figure 4 presents relevant pictures of these experiments, including intra-vegetation *P. aeruginosa* in untreated rats (Figure 4.A and 4.B), negatively stained phages from the cocktail with a capsid size of ca. 70 nm (Figure 4.C), and intra-vegetation lysed bacteria in phage treated rats with bacterial ghosts containing phage particles (Figure 4.D).

Correlation between phage multiplication, antimicrobial activity, and cytokine production. *In vivo* antibacterial activity correlated with phage amplification (ca. 3 log PFU/g of vegetations) after both continuous and bolus injection (Figure 3.C). This relation was further underlined by the scatter plot presented in Figure 3.D, which showed a significant inverse correlation between phage and bacterial concentrations in the vegetations (correlation value (r); -0.66, Pearson two tailed correlation test; $p = 0.003$).

Successful phage therapy also correlated with the production of specific inflammatory cytokines (Figure 5). Concentrations of IL-1 β , IL-6 and TNF α in plasma were quantified by Luminex first before inoculation, second before treatment onset, and lastly after 6 h of phage therapy in uninfected and infected rats (Figure 5.A). Several observations were drawn from these measurements. First, although there were trends in cytokine-induction by bacteria and phages alone, these were not statistically significant. Second, TNF α levels remained essentially unaltered in all of the groups throughout the experiment. Finally, only phages treatment, but not ciprofloxacin, significantly increased plasma levels of IL-1 β and IL-6 (Figure 5.B). Since ciprofloxacin is not bacteriolytic, the increase in IL-1 β and IL-6 levels was likely related to phage-induced bacterial lysis.

Phage resistance in EE. Since spontaneous phage-resistant mutants occurred at a rate of 10^{-7} in batch cultures and fibrin clots, they were also expected to emerge in infected vegetations. To test this assumption, phage-resistant mutants were sought in infected valves by plating vegetation extracts directly on agar plates containing pre-adsorbed phages. Unexpectedly, no phage-resistant mutants could be isolated from the infected vegetations either before or after therapy, therefore suggesting that phage resistance might result in altered virulence or fitness and interfere with successful bacterial survival or growth *in vivo*. Two resistant isolates recovered from fibrin clots, 19/2 and 24/2, which showed different phage resistance patterns, were further characterized to verify this hypothesis. Figure 6.A shows that these resistant isolates had markedly different phage susceptibility profiles when compared to the parent strain. Mutant 24/2 conferred turbid plaques while the mutant 19/2 was

resistant to 10 of the 12 phages and displayed a melanized (dark colonies) phenotype.

To determine whether these mutants had altered virulence, they were tested for their capability to infect sterile vegetations. A single bolus of 10^8 CFU (*i.e.* infective dose 90% (ID 90) of parent strain) led to the infection of < 60 % ($p < 0.05$) and < 30 % ($p < 0.01$) of vegetations for mutants 19/2 and 24/2, respectively (Figure 6.B). Moreover, the median bacterial densities in the infected vegetations were significantly lower than in rats infected with the parent strain (CHA, 8.9 CFU/g; 24/2, 7.3 CFU/g; and 19/2, 6.8. $p < 0.05$) and blood cultures were negative.

To further investigate the origin of this impaired *in vivo* infectivity the genomic DNA of the parent strain CHA and the two mutants was sequenced, assembled, and compared (Figure 7.A). Mutant 24/2 displayed a 15 bp deletion at the 3' end of the *pilT* gene (Supplementary Figure 4), which encodes an ATPase involved in motility [17]. As a result, mutant 24/2 exhibited loss of twitching motility (Figure 7.B). Mutant 19/2 had a 362 kb genomic deletion encompassing 342 genes. These included the *galU* gene, which is involved in *P. aeruginosa* LPS core synthesis. *galU*-deletion was shown to be responsible for phage resistance [18]. The resulting absence of O-antigen and LPS core truncation was confirmed by LPS extraction followed by gel electrophoresis (Figure 7.C). Mutant 19/2 also showed a 3-fold decrease in its MIC of ciprofloxacin (0.064 vs 0.192 $\mu\text{g/ml}$ for mutant 19/2 and parent CHA, respectively).

Discussion

While phage therapy is a promising alternative to antibiotics against specific and difficult-to-treat infections, careful appraisal of its therapeutic potential is an absolute prerequisite before clinical application.

Here we evaluated the *in vitro* activity of the whole phage cocktail and its individual phage components against a panel of independent *P. aeruginosa* isolates in test tubes and in fibrin clots. This revealed the presence of bacterial strains with opposite susceptibility profiles, either resistant to all the cocktail's phages (e.g. strain PA7) or susceptible to all of them (e.g. strain CHA). The frequency of spontaneous phage resistance mutations of the susceptible strain CHA was found to be of ca. 10^{-7} . This predicted that phage resistance would emerge in infected fibrin clots, which contained $\geq 10^8$ CFU/g. This was indeed the case. However these approach experiments highlighted two additional important facts. First, phages could readily diffuse into clots, kill the overwhelming majority of phage-susceptible bacteria *in situ*, and protect the fibrin matrix from bacterial-induced disintegration. Second, combining phages with low concentrations of ciprofloxacin or meropenem (2.5 x the MIC) inhibited the regrowth of phage-resistant mutants, suggesting potential success of *in vivo* therapy. The *in vivo* experiments provided further critical information. Regarding PK/PD parameters, phages were relatively stable in plasma (elimination half-life of ca. 2.3 h following bolus administration) and persisted longer in organs (half-life up to 9 h). These values were consistent with those observed in previous work [19] and confirmed that phages, whose sizes vary from ca. 50 to 200 nm, can diffuse into various body compartments [5, 6, 20]. As a result, phages were able to kill bacteria inside valve vegetations and multiply locally by up to 3 log PFU/g within 6 h. Phage-induced killing correlated with a burst of IL-1 β and IL-6. Since cytokine levels were

measured only at a single time point, the data did not permit extrapolating the dynamics of cytokine responses over time. However, the significant increase in IL-1 β and IL-6 levels in rats treated with phages – as compared to rats treated with ciprofloxacin – most likely reflected the release of cell debris by phage-mediated lysis. Accordingly, it is known that both cytokines are inducible by LPS [21] and that similar results were obtained in EE using a bactericidal phage lysin [22].

From a therapeutic point of view, the combination of phages with ciprofloxacin exhibited a highly synergistic effect and resulted in 7/11 (64%) negative valve cultures within 6 h. This remarkable result has no precedent in antimicrobial therapy of EE with virtually any drug or pathogen, and especially not with *P. aeruginosa* [23-25].

Phage-antibiotic (or PAS) synergism has been formerly reported [26-29]. The mechanism of PAS is proposed to result from antibiotic-induced bacterial elongation, which may facilitate the access of phages to their bacterial target [29]. However, none of the previous PAS studies were done *in vivo* and none of them demonstrated the extensive killing of > 7 orders of magnitude in 6 h reported herein [26-29]. Interestingly, phage-resistant subpopulations were readily detected in broth cultures and infected clots, but not in vegetations. This suggests that preexisting phage-resistant mutants might be hampered *in vivo*, as proposed by others [6, 11, 12, 30, 31].

In fact, the mutations that conferred resistance to the phage cocktail came at a great physiological cost. The present experiments provide two examples supporting this notion. Mutant 24/2 exhibited defective cell motility due to disruption of the *pilT* gene, whose product is an ATPase providing energy for type IV pilus contraction and bacterial twitching [17]. Type IV pilus is also a phage receptor and pilus contraction is

believed to bring the phages closer to the bacterial envelope [32]. Mutant 19/2 had a truncated LPS resulting from a large deletion encompassing the *galU* gene involved in the synthesis of the LPS core [18, 33]. LPS can also act as a phage receptor and its alteration can confer phage resistance [13]. Both type IV pili and LPS are major virulence factors in *P. aeruginosa* and their mutation can result in attenuated virulence [13, 34]. Thus, while these mutations confer resistance to phages, they may also decrease fitness in animals, while preserving normal growth in less stringent *in vitro* conditions.

While these observations are promising regarding phage antibacterial activity, caution should be raised as to the use of phage cocktails versus single phage preparations. While, phage cocktails provide broader strain coverage than single phages, they also carry greater risks of unwanted gene transfer and inter-phage interference. Ideally phages should be tailored against their target pathogen and specificity should be preferred to exhaustiveness, just like for antibiotic therapy.

Altogether the present results provide a strong proof-of-concept for phage therapy of deep-seated and systemic infections. Moreover they raise the provocative possibility that certain infections might be cured by a single phage injection most efficiently combined with synergistic antibiotics. Indeed, once locally established phages can multiply *in situ* and do not necessitate further administration.

Methods

Strains, phage cocktail and antibiotics. A total of 33 *P. aeruginosa* reference strains and clinical isolates from our own clinical strain collection were used in *in vitro* susceptibility determinations (Supplementary Table 1). These isolates were not meant cover the diversity of contemporary pseudomonas from our hospitals, but to select strains with extreme phenotypes to be tested in the present experiments. Growth conditions and reagents are given in the supplementary material.

***In vitro* studies.** The host range of the individual phages composing the PP1131 cocktail was determined using spot or plaque assays [35]. Experiments were done in triplicates. Plasma clots were prepared in 96-well microplates, as previously described [15]. Phage titers were measured by plaque assays [35]. The activity of the phage cocktail was considered bactericidal when it killed ≥ 3 log CFU of the starting inoculum in the clot. Details are provided in the supplementary materials.

Animal studies. Experiments were approved by and in adherence with the guidelines of the Swiss Animal Protection Law, Veterinary office, State of Vaud. Experiments were performed under license number 879.9 and in accordance with the regulations of the cantonal committee on animal experimentation of the State of Vaud, Switzerland. The production of catheter-induced aortic vegetations and the installation of an i.v. line into the superior vena cava, connected to an infusion pump to deliver the phage cocktail, were performed in female Wistar rats as previously described [16]. Details are provided in the supplementary materials.

Histology. Semi-thin and ultra-thin sections were prepared as described in [36] and cut with a Leica Ultracut microtome (Leica Mikrosysteme GmbH, Vienna, Austria). Sections were stained for light microscopy using the modified Brown and Brenn method, as described in [37]. Ultra-thin sections of 50 nm were stained as described in. For phage observation, phage cocktail was adsorbed on copper 200-mesh grid coated with Formvar-carbon (EMS) and stained with uranyl acetate. Micrographs were taken with a transmission electron microscope FEI CM100 (FEI, Eindhoven, the Netherlands) at an acceleration voltage of 80 kV with a TVIPS TemCam-F416 digital camera (TVIPS GmbH, Gauting, Germany).

Cytokine measurements. The serum inflammatory cytokines IL-1 β , IL-6 and TNF α were quantified prior to infection (24 h after surgery), prior to therapy (18 h after bacterial inoculation) and at sacrifice (6 h after onset of therapy). Plasma was kept at -80°C and cytokines titers were using the Biorad Bio-Plex Rat Cytokine Kit in a Luminex 200 system and following manufacturer's recommendations (done by MEF; University of Lausanne, Switzerland).

Detection and characterization of phage resistance. Phage resistant bacteria were isolated from broth cultures, *in vitro* fibrin clots, and rat vegetations by plating on blood agar plates containing 10¹⁰ PFU pre-absorbed phages. Resistance rates were determined as the number of bacteria growing on plates pre-adsorbed with phages divided by the number of bacteria growing on plain plates. *In vivo* infectivity of phage resistant was assessed by inoculating rats with catheter-induced aortic vegetations as previously described. Full genomic DNA sequencing was performed by the Center for Integrative Genomics (CIG; University of Lausanne, Switzerland) using the Pacific

Biosciences RSII platform (Pacific Bioscience, Menlo Park, CA). Total DNA was extracted using the DNeasy Blood and Tissue kit (Qiagen, Valencia, CA, USA) according to manufacturer's instructions. GenDB [38], BLASTn [39], and BRIG [40] were used for genomic analysis. Subsurface twitching motility tests were performed as described [41]. LPS was extracted using the iNTRON LPS extraction kit (iNtRON biotechnology, Daejeon, South Korea), resolved on NuPAGE 4-12% BisTris gels (Invitrogen, Carlsbad, CA, USA), and silver stained according to [42]. Details are provided in the supplementary materials.

Notes

Acknowledgments. We are indebted to Marlyse Giddey, Matthew Parkan, Sara Mitri, Glib Mazepa, Shawna McCallin, Jean Daraspe and Gilles Willemen for their invaluable technical support and fruitful discussions.

Financial support. This work was supported in part by the Swiss National Research Foundation (CR31I3_166124, 310030-143799) (YAQ, JME) and the European Commission research grant (FP7-PHAGOBURN) (YAQ). This work was also supported by a non-restricted grant from the Loterie Suisse Romande (YAQ). The funders had no role in study design, data collection and interpretation, or the decision to submit the work for publication.

Potential conflict of interest. Jérôme Gabard is employed by the commercial company Pherecydes Pharma as COO. The bacteriophage cocktail PP1131 used in this study is produced under license by the company Pherecydes Pharma and used

in a human clinical trial (Phagoburn, NCT02116010, <http://www.phagoburn.eu/>). Yok-Ai Que is co-investigator in the clinical trial Phagoburn, which uses the PP1131 bacteriophage cocktail.

Correspondence. Please address correspondence to Frank Oechslin, Frank.Oechslin@gmail.ch. University of Lausanne, Quartier UNIL-Sorge, Bâtiment Biophore, CH-1015 Lausanne, Switzerland.

Accepted Manuscript

References

1. Chanishvili N. Phage therapy--history from Twort and d'Herelle through Soviet experience to current approaches. *Adv Virus Res* **2012**; 83:3-40.
2. Abedon ST. Phage therapy of pulmonary infections. *Bacteriophage* **2015**; 5:e1020260.
3. Lang G, Kehr P, Mathevon H, Clavert JM, Sejourne P, Pointu J. [Bacteriophage therapy of septic complications of orthopaedic surgery (author's transl)]. *Rev Chir Orthop Reparatrice Appar Mot* **1979**; 65:33-7.
4. Speck P, Smithyman A. Safety and efficacy of phage therapy via the intravenous route. *FEMS Microbiol Lett* **2016**; 363.
5. Chhibber S, Kaur S, Kumari S. Therapeutic potential of bacteriophage in treating *Klebsiella pneumoniae* B5055-mediated lobar pneumonia in mice. *J Med Microbiol* **2008**; 57:1508-13.
6. Pouillot F, Chomton M, Blois H, et al. Efficacy of bacteriophage therapy in experimental sepsis and meningitis caused by a clone O25b:H4-ST131 *Escherichia coli* strain producing CTX-M-15. *Antimicrob Agents Chemother* **2012**; 56:3568-75.
7. Marza JA, Soothill JS, Boydell P, Collins TA. Multiplication of therapeutically administered bacteriophages in *Pseudomonas aeruginosa* infected patients. *Burns* **2006**; 32:644-6.
8. Wright A, Hawkins CH, Anggard EE, Harper DR. A controlled clinical trial of a therapeutic bacteriophage preparation in chronic otitis due to antibiotic-resistant *Pseudomonas aeruginosa*; a preliminary report of efficacy. *Clin Otolaryngol* **2009**; 34:349-57.
9. Rhoads DD, Wolcott RD, Kuskowski MA, Wolcott BM, Ward LS, Sulakvelidze A. Bacteriophage therapy of venous leg ulcers in humans: results of a phase I safety trial. *J Wound Care* **2009**; 18:237-8, 40-3.
10. Labrie SJ, Samson JE, Moineau S. Bacteriophage resistance mechanisms. *Nat Rev Microbiol* **2010**; 8:317-27.
11. Lenski RE. Experimental studies of pleiotropy and epistasis in *Escherichia coli* variation in competitive fitness among mutants resistant to virus T4. *Evolution* **1988**; 42:425-32.
12. Scanlan PD, Buckling A, Hall AR. Experimental evolution and bacterial resistance: (co)evolutionary costs and trade-offs as opportunities in phage therapy research. *Bacteriophage* **2015**; 5:e1050153.
13. Le S, Yao X, Lu S, et al. Chromosomal DNA deletion confers phage resistance to *Pseudomonas aeruginosa*. *Sci Rep* **2014**; 4:4738.
14. Que YA, Moreillon P. Infective endocarditis. *Nature reviews Cardiology* **2011**; 8:322-36.
15. Entenza JM, Haldimann A, Giddey M, Lociuro S, Hawser S, Moreillon P. Efficacy of iclaprim against wild-type and thymidine kinase-deficient methicillin-resistant *Staphylococcus aureus* isolates in an in vitro fibrin clot model. *Antimicrob Agents Chemother* **2009**; 53:3635-41.
16. Entenza JM, Vouillamoz J, Glauser MP, Moreillon P. Levofloxacin versus ciprofloxacin, flucloxacillin, or vancomycin for treatment of experimental endocarditis due to methicillin-susceptible or -resistant *Staphylococcus aureus*. *Antimicrob Agents Chemother* **1997**; 41:1662-7.

17. Mattick JS. Type IV pili and twitching motility. *Annu Rev Microbiol* **2002**; 56:289-314.
18. Dean CR, Goldberg JB. *Pseudomonas aeruginosa* galU is required for a complete lipopolysaccharide core and repairs a secondary mutation in a PA103 (serogroup O11) wbpM mutant. *FEMS Microbiol Lett* **2002**; 210:277-83.
19. Merrill CR, Biswas B, Carlton R, et al. Long-circulating bacteriophage as antibacterial agents. *Proc Natl Acad Sci U S A* **1996**; 93:3188-92.
20. Gorski A, Wazna E, Dabrowska BW, Dabrowska K, Switala-Jelen K, Miedzybrodzki R. Bacteriophage translocation. *FEMS Immunol Med Microbiol* **2006**; 46:313-9.
21. de Bont N, Netea MG, Rovers C, et al. LPS-induced release of IL-1 beta, IL-1Ra, IL-6, and TNF-alpha in whole blood from patients with familial hypercholesterolemia: no effect of cholesterol-lowering treatment. *J Interferon Cytokine Res* **2006**; 26:101-7.
22. Entenza JM, Loeffler JM, Grandgirard D, Fischetti VA, Moreillon P. Therapeutic effects of bacteriophage Cpl-1 lysin against *Streptococcus pneumoniae* endocarditis in rats. *Antimicrob Agents Chemother* **2005**; 49:4789-92.
23. Papadakis JA, Samonis G, Maraki S, Boutsikakis J, Petrocheilou V, Saroglou G. Efficacy of amikacin, ofloxacin, pefloxacin, ciprofloxacin, enoxacin and fleroxacin in experimental left-sided *Pseudomonas aeruginosa* endocarditis. *Chemotherapy* **2000**; 46:116-21.
24. Bayer AS, Norman D, Kim KS. Efficacy of amikacin and ceftazidime in experimental aortic valve endocarditis due to *Pseudomonas aeruginosa*. *Antimicrob Agents Chemother* **1985**; 28:781-5.
25. Robaux MA, Dube L, Caillon J, et al. In vivo efficacy of continuous infusion versus intermittent dosing of ceftazidime alone or in combination with amikacin relative to human kinetic profiles in a *Pseudomonas aeruginosa* rabbit endocarditis model. *J Antimicrob Chemother* **2001**; 47:617-22.
26. Ryan EM, Alkawareek MY, Donnelly RF, Gilmore BF. Synergistic phage-antibiotic combinations for the control of *Escherichia coli* biofilms in vitro. *FEMS Immunol Med Microbiol* **2012**; 65:395-8.
27. Knezevic P, Curcin S, Aleksic V, Petrusic M, Vlaski L. Phage-antibiotic synergism: a possible approach to combatting *Pseudomonas aeruginosa*. *Res Microbiol* **2013**; 164:55-60.
28. Kamal F, Dennis JJ. Burkholderia cepacia complex Phage-Antibiotic Synergy (PAS): antibiotics stimulate lytic phage activity. *Appl Environ Microbiol* **2015**; 81:1132-8.
29. Comeau AM, Tetart F, Trojet SN, Prere MF, Krisch HM. Phage-Antibiotic Synergy (PAS): beta-lactam and quinolone antibiotics stimulate virulent phage growth. *PLoS One* **2007**; 2:e799.
30. Scanlan PD, Hall AR, Blackshields G, et al. Coevolution with bacteriophages drives genome-wide host evolution and constrains the acquisition of abiotic-beneficial mutations. *Mol Biol Evol* **2015**; 32:1425-35.
31. Smith HW, Huggins MB, Shaw KM. The control of experimental *Escherichia coli* diarrhoea in calves by means of bacteriophages. *Journal of general microbiology* **1987**; 133:1111-26.
32. Bradley DE. Shortening of *Pseudomonas aeruginosa* pili after RNA-phage adsorption. *Journal of general microbiology* **1972**; 72:303-19.
33. Rodriguez-Rojas A, Mena A, Martin S, Borrell N, Oliver A, Blazquez J. Inactivation of the hmgA gene of *Pseudomonas aeruginosa* leads to pyomelanin hyperproduction, stress resistance and increased persistence in chronic lung infection. *Microbiology* **2009**; 155:1050-7.

34. Comolli JC, Hauser AR, Waite L, Whitchurch CB, Mattick JS, Engel JN. *Pseudomonas aeruginosa* gene products PilT and PilU are required for cytotoxicity in vitro and virulence in a mouse model of acute pneumonia. *Infect Immun* **1999**; 67:3625-30.
35. Clokie MRJ, Kropinski AM. *Bacteriophages. Methods and Protocols. Volume 1: Isolation, Characterization, and Interactions.* Humana Press ed. Vol. 1. **2009**.
36. Broskey NT, Daraspe J, Humbel BM, Amati F. Skeletal muscle mitochondrial and lipid droplet content assessed with standardized grid sizes for stereology. *Journal of applied physiology (Bethesda, Md : 1985)* **2013**; 115:765-70.
37. Taylor RD. Modification of the Brown and Brenn gram stain for the differential staining of gram-positive and gram-negative bacteria in tissue sections. *Am J Clin Pathol* **1966**; 46:472-4.
38. Meyer F, Goesmann A, McHardy AC, et al. GenDB--an open source genome annotation system for prokaryote genomes. *Nucleic Acids Res* **2003**; 31:2187-95.
39. Altschul SF, Gish W, Miller W, Myers EW, Lipman DJ. Basic local alignment search tool. *J Mol Biol* **1990**; 215:403-10.
40. Alikhan NF, Petty NK, Ben Zakour NL, Beatson SA. BRIG: simple prokaryote genome comparisons. *BMC Genomics* **2011**; 12:402.
41. Semmler AB, Whitchurch CB, Mattick JS. A re-examination of twitching motility in *Pseudomonas aeruginosa*. *Microbiology* **1999**; 145 (Pt 10):2863-73.
42. Zhu ZX, Cong WT, Ni MW, et al. An improved silver stain for the visualization of lipopolysaccharides on polyacrylamide gels. *Electrophoresis* **2012**; 33:1220-3.

Figure legends

Figure 1. Activity of phage cocktail PP1131 in *in vitro* fibrin clots. Clots were produced from rat plasma and infected with 10^8 CFU/ml of either phage-resistant *P. aeruginosa* strain PA7 (A) or phage-susceptible strain CHA (B). Clots were left untreated (solid lines) or exposed to 10^8 PFU/ml of PP1131 for 24 h at 37°C (dashed lines). Phage titers in non-infected clots (solid lines) and in PA7-infected or CHA-infected clots (dashed lines) were determined 6 h and 24 h after exposure to the phage cocktail. Clots infected with strain PA7 lysed in spite of phage treatment (C), whereas those infected with phage-susceptible CHA and treated with phages remained intact (D). *p*-values were determined using the Mann Whitney test.

Figure 2. Bactericidal synergism between phages and selected antibiotics. Bacterial killing by phage-antibiotic combinations was tested by using 10^8 PFU/ml of PP1131 with 2.5-times the MIC of ciprofloxacin (A) or meropenem (B) (MIC of 0.19 µg/ml and 0.125 µg/ml, respectively). Each value represents the mean ± SD of 4 to 16 independent clots. ABT; antibiotic.

Figure 3. PK/PD and therapeutic efficacy of phage cocktail PP1131 and ciprofloxacin in rats with EE due to *P. aeruginosa* CHA. (A) Pharmacokinetics in the absence of infection of phage cocktail PP1131 in rat plasma after either a single i.v. bolus injection (1 ml of 10^{10} PFU/ml in 1 min, dashed line, Bolus) or the same amount of phages administered through continuous infusion (0.1 ml/h of 10^{10} PFU/ml over 24 h, solid line, C.I.). Each value represents the mean ± SD from 8 to 10 individual animals. (B) Bacterial loads of infected vegetations after 6 h of phage treatment administered through continuous infusion or in single bolus, and treatment

with ciprofloxacin alone or combined with phages. Each dot represents the vegetation of a single animal. The mode of injection and type of treatment are indicated at the top of columns (C.I.; continuous infusion. ϕ ; phages). Statistical results are indicated at the bottom of columns (\dagger : control versus all types of treatment, $p < 0.0005$. \ddagger : combination versus control and all the other types of treatments, $p < 0.0001$; results were compared by the Mann Whitney test). (C) Phage titers in vegetations measured in uninfected rats treated with bolus phage injection (control) or infected rats treated with the same regimens as in Fig 2.B (***, $p < 0.0001$ using the Mann Whitney test). (D) Correlation between the decrease in vegetation bacterial loads and the vegetation phage titers resulting from *in situ* phage amplification (continuous infusion and bolus injection pooled together; correlation value (r): -0.66, Pearson two tailed correlation test: $p = 0.003$). cip: ciprofloxacin.

Figure 4. Light microscopy and TEM of rat vegetations after 6 h phage therapy.

(A) Semi-thin section (200 nm) of control vegetation infected with *P. aeruginosa* CHA stained using the modified Braun Brenn staining protocol [37]. Arrows indicate bacteria, stained in red (RBC: red blood cells). (B) TEM of ultra-thin sections (50 nm) of control vegetation infected with *P. aeruginosa* CHA positive-stained using uranium acetate and lead citrate. Arrows indicate bacteria. (C) Example of a negative staining of a myoviridae phage present in the cocktail; other phages morphotypes including podoviridae were also present. (D) TEM of vegetation infected by *P. aeruginosa* CHA and treated with the phage cocktail. Arrows indicate phage capsids inside lysed bacteria.

Figure 5. Cytokine quantification in rat plasma during EE. (A) Protocol of blood sampling for cytokine quantification. (B) Levels of IL-1 β , IL-6 and TNF- α measured after 6 h of phage or antibiotherapy (treatment). Controls included rats 24 h after surgery (inoculum, T0), untreated but infected rats for 18 h or 24 h (bacteria T18 and T24), and uninfected rats receiving phage for 6 h (Phages T6). Each value represents the mean \pm SEM from 4 to 10 individual animals (*, $p = 0.03$ and **, $p = 0.005$ using the Mann Whitney test). cip: ciprofloxacin.

Figure 6. Infectivity of phage-resistant *P. aeruginosa* mutants in rats with catheter-induced vegetations. (A) Two phage resistant *P. aeruginosa* mutants, 24/2 and 19/2, were isolated *in vitro* from fibrin clots and showed different phage resistance patterns. Lysis zones at the site of the phage deposits indicated phage-sensitivity. The absence of lysis indicated phage-resistance. (B) The isolates' infectivity was tested in rats with catheter-induced vegetations. Both variants showed a loss of infectivity (>40 % for 24/2 and >70 % for 19/) as compared to the parent strain CHA. p -values were determined using Fisher's exact test.

Figure 7. Characterization of phage-resistant *P. aeruginosa* mutants. The two phage resistant *P. aeruginosa* mutants, 24/2 and 19/2, isolated *in vitro* were further characterized regarding to genomic content and phenotypes. (A) Variant 24/2 displayed a 15 bp deletion in the *pilT* gene and variant 19/2 displayed a 362 Kb chromosomal deletion that encompassed the *galU* gene. (B) Impaired twitching motility resulting from the *pilT* alteration in variant 24/2, as compared to wild type PAO1 and parent CHA. (C) Impaired LPS synthesis resulting from the *galU* deletion in variant 19/2 with absence of O-antigen (O) and LPS core (C), as compared to parent CHA.

Figure 1

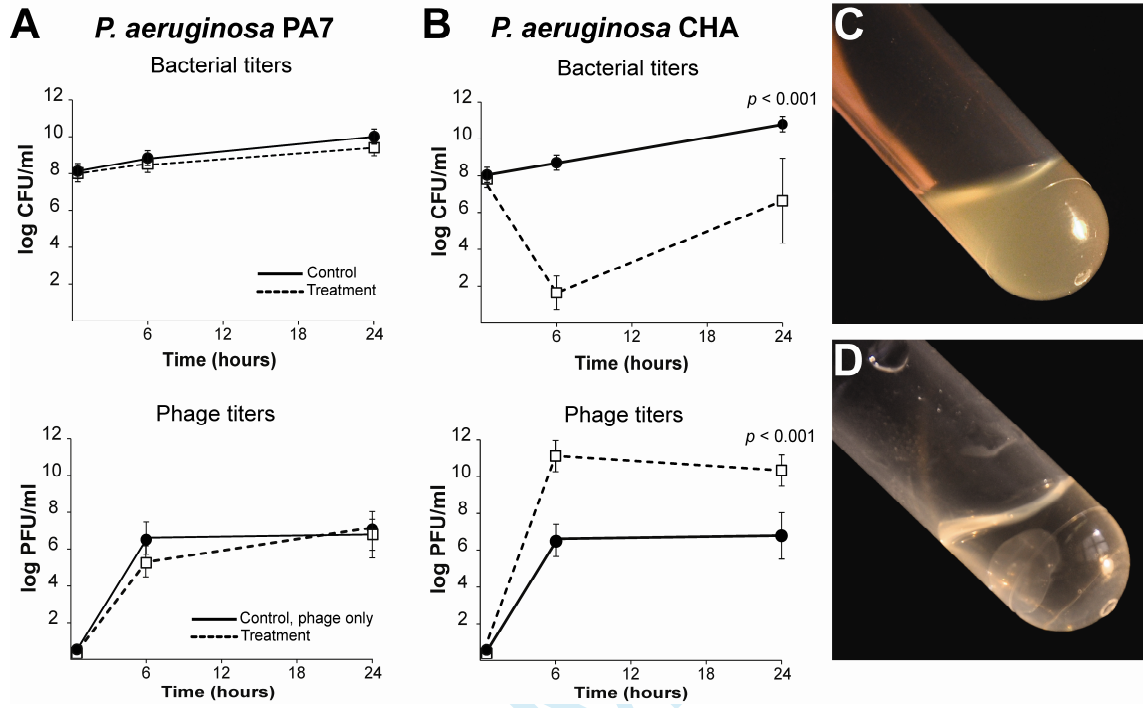


Figure 2

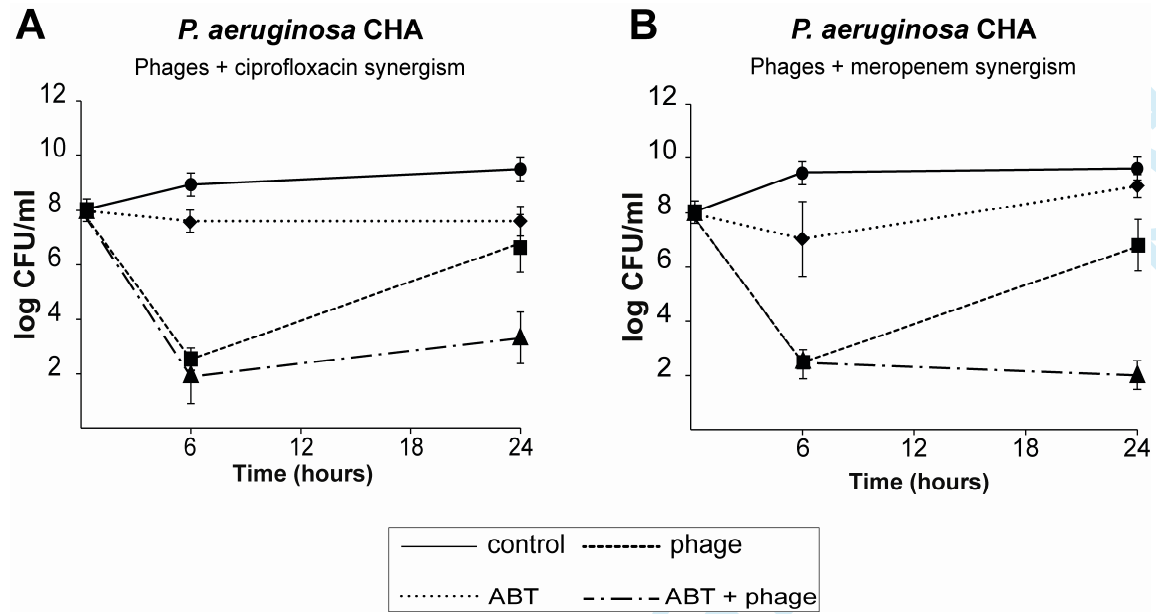


Figure 3

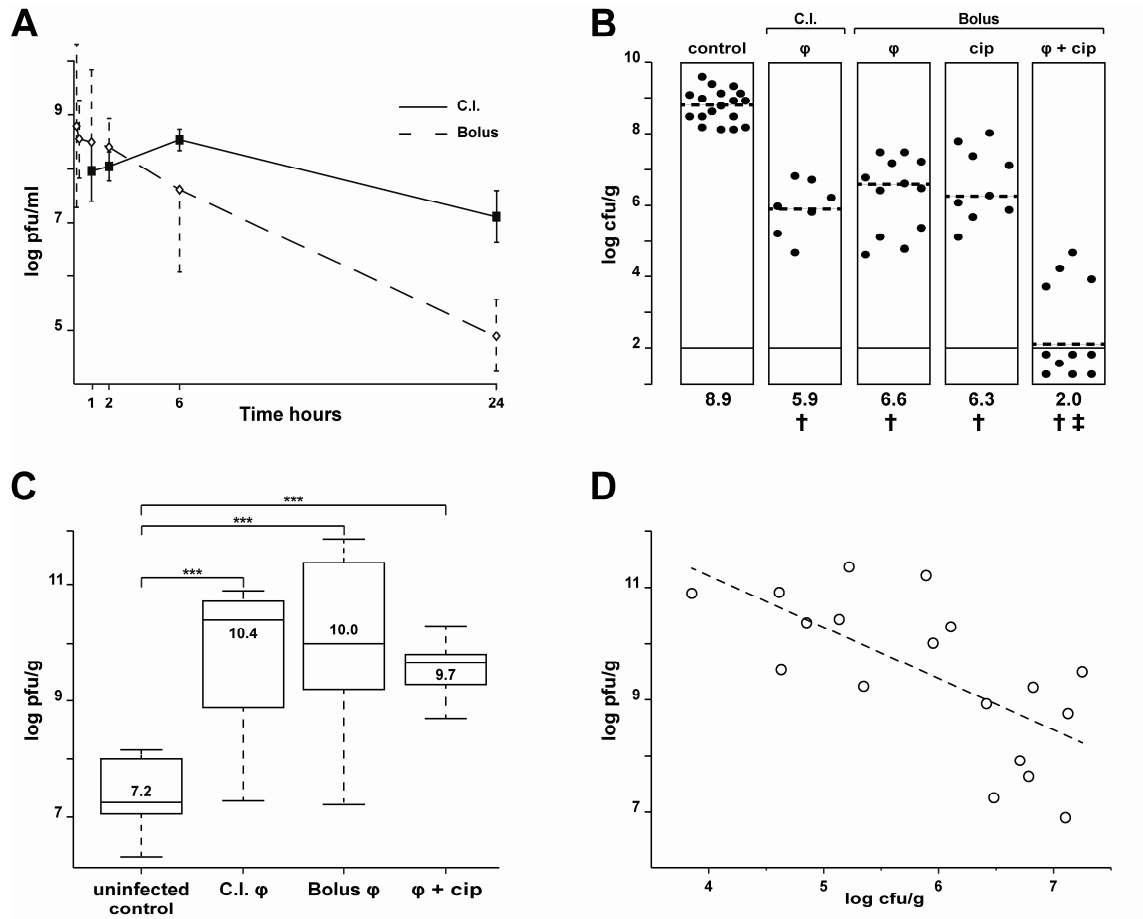


Figure 4

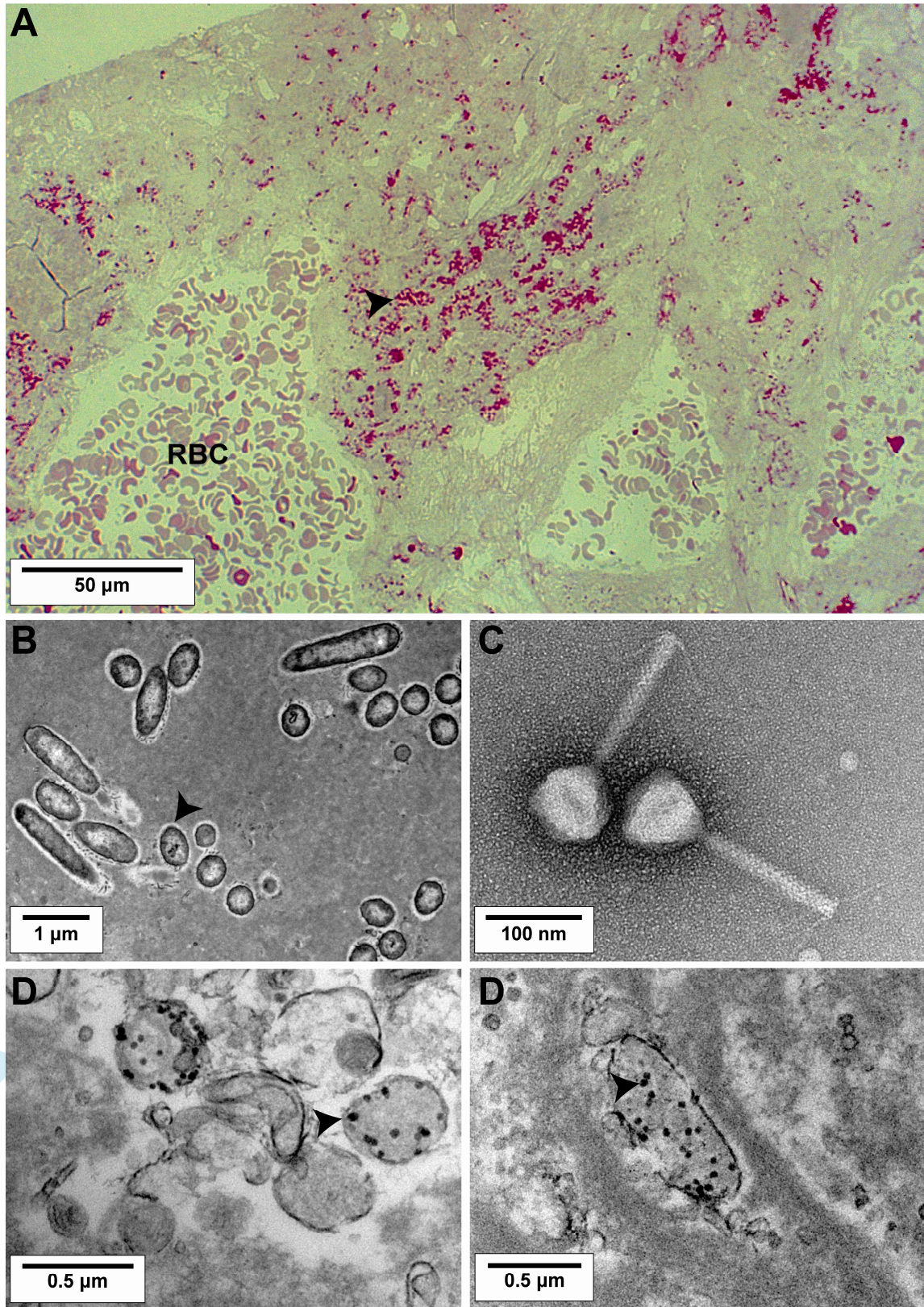


Figure 5

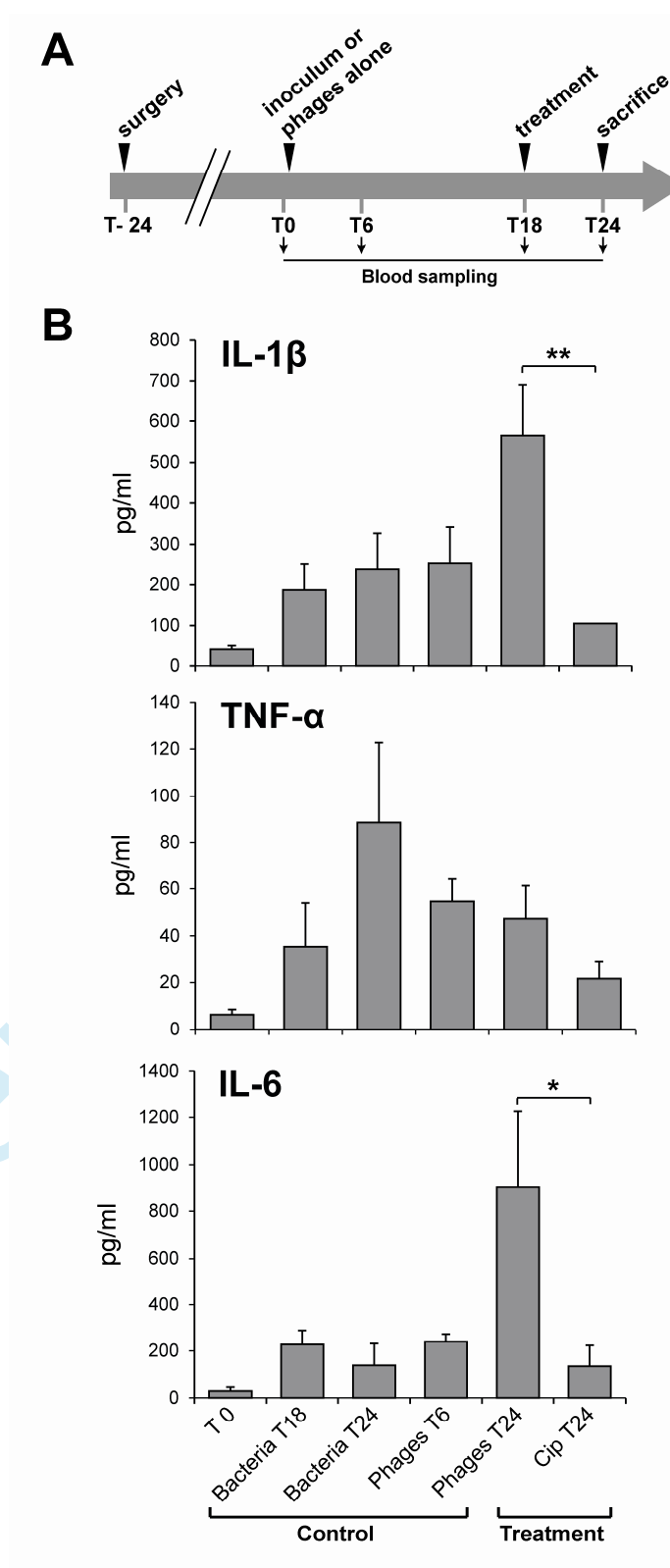


Figure 6

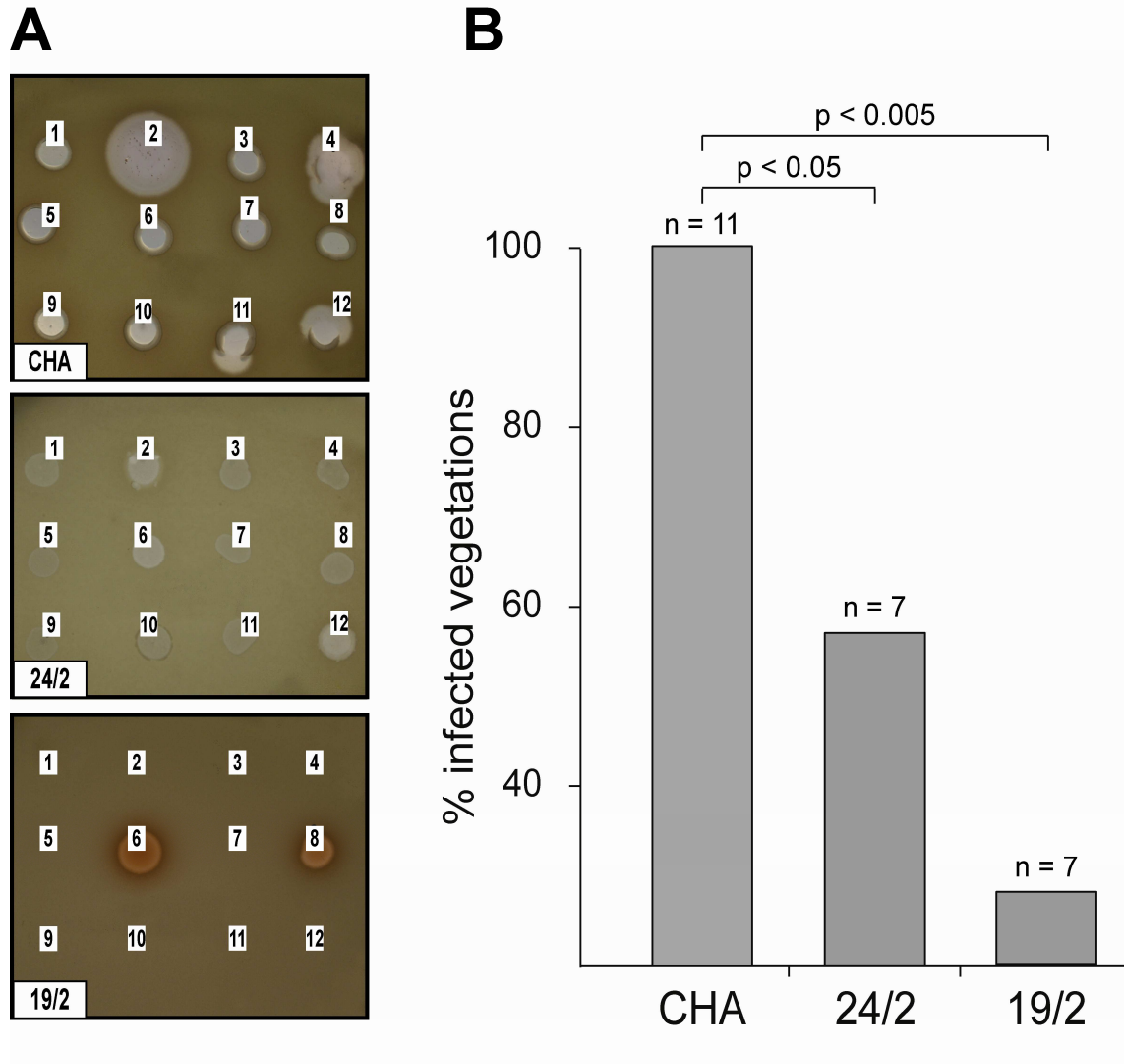


Figure 7

